Studies on the Light-Focusing Plastic Rod. XIII. Photocopolymerization of Methyl Methacrylate–Vinyl Esters of Aromatic Carboxylic Acid

YASUHIRO KOIKE, YOSHIHIKO KIMOTO, and YASUJI OHTSUKA,
Department of Applied Chemistry, Faculty of Science and Technology, Keio University, 3-14-1 Hiyoshi, Kohoku-ku, Yokohama-shi, 223, Japan

Synopsis

The light-focusing plastic rod (LFR) was prepared by the photocopolymerization of methyl methacrylate (MMA) with vinyl phenylacetate (VPAc) and vinyl benzoate (VB), using benzoyl peroxide (BPO), benzoin (BN), and benzoin methyl ether (BME) as an initiator. The LFR with high transparency and steep refractive-index distribution was obtained using the MMA–VPAc pair and the BME. The difference in the index distributions under BPO, BN, and BME initiations was clarified in terms of the photoinitiation rate and the accompanying thermal polymerization during the photocopolymerization process. The light scattering intensity from the LFR was related to the heterogeneity of the copolymer composition and the compatibility between the M_1 and M_2 polymers. The comparison of the light scattering theory with the experimental data indicated that the much less scattering intensity from the MMA–VPAc LFR than the MMA–VB LFR should be attributed to the good compatibility between the MMA and VPAc polymers, and scarcely attributed to the index difference between the VPAc and VB polymers.

INTRODUCTION

The gradient-index (GRIN) optics[1,2] have been rapidly advanced, being expected for imaging system,[3,4] fiber coupling,[5] switches, and multiplexers,[6] etc. A GRIN cylindrical rod has the convex-lens characteristics, in which the refractive-index distribution is expressed as

$$\begin{aligned} n(r) &= n_0(1 - \tfrac{1}{2}A \cdot r^2) \\ &= n_0[1 - \tfrac{1}{2}A' \cdot (r/R_p)^2] \end{aligned} \tag{1}$$

where n_0 is the refractive index at the center axis, $n(r)$ is the refractive index at a distance r from the center axis, R_p is the radius of the rod, and A or A' ($\equiv A \cdot R_p^2$) is a constant of the refractive-index distribution. Concerning glass GRIN rod, the Selfoc[7] rod lens has been currently manufactured by ion exchange of a Thallium- or Cesium-based glass rod.

We had reported that a plastic GRIN rod lens (designated as a light-focusing plastic rod, LFR, by us) could be fabricated by two different processes, namely by two-step copolymerization[8–11] and by photocopolymerization.[12–14] The former process yielded the plastic GRIN-rod lens with excellent convex-lens function and low chromatic aberration. On the other hand, the LFR from the latter process is capable of heat-drawing into a light-focusing plastic fiber[15] (LFF) because of its linear structure. The resulting LFF will be available for a short-distance telecommunication fiber and for a GRIN-fiber lens.

In this paper, the plastic GRIN rod was prepared by the photocopolymeriza-

Journal of Applied Polymer Science, Vol. 27, 3253–3264 (1982)
 CCC 0021-8995/82/093253-12$02.20

tion of methyl methacrylate (MMA) with vinyl phenylacetate (VPAc) and vinyl benzoate (VB), using benzoyl peroxide (BPO), benzoin (BN), and benzoin methyl ether (BME) as an initiator. The MMA–VPAc LFR had much higher transparency than that of the MMA–VB LFR. Using BME led to the steeper refractive-index distribution than using BN or BPO as an initiator. We have focused on relating the light scattering of the LFR to the heterogeneity of the chemical structure and clarifying the effect of the initiation on the mechanism forming a radial refractive-index distribution.

EXPERIMENTAL

Materials

MMA (reagent grade) was distilled under reduced pressure after removing an inhibitor with aqueous 0.5*N* NaOH solution and washing with distilled water five times. VPAc and VB were synthesized according to the vinylation[16] of phenylacetic acid and benzoic acid with acetylene, using mercuric acetate as a catalyst, and then distilled at bp 64°C/4.0 Torr and at bp 70°C/3.5 Torr, respectively. BPO, BME, and BN were recrystallized from chloroform-cold methanol, *n*-hexane, and chloroform-cold ethanol, respectively.

Fabrication of LFR

The detail of the photocopolymerization procedure was already reported in Ref. 12. The pair of M_1 and M_2 monomers in the photocopolymerization process should satisfy the following items: When the refractive index of the M_1 homopolymer is lower than that of the M_2 homopolymer, the monomer reactivity ratio r_1 is greater than unity and r_2 is less than unity. As shown in Table I, the monomer pairs of MMA–VPAc and MMA–VB are suitable to this process.

The mixture of M_1 and M_2 monomers containing a specified amount of an initiator was filled in a glass tube with a 3-mm inner diameter (9-mm diameter for the sample of light scattering). Rotating the glass tube on its axis, it was exposed to UV light (Toshiba high-pressure mercury vapor lamp H400P) from the side, while the UV source was moved upward with a constant velocity V (=0.3–0.9 mm/min in this paper). The chamber was air-cooled at 25°C during the UV irradiation. The copolymer layer is formed on the inner wall of the glass tube, and the thickness of the layer increases with irradiation time until the content of the glass tube is solidified to the center axis. A copolymer formed in the initial stage (i.e., on the inner wall of the glass tube) is rich in M_1 unit because $r_1 > 1$ and $r_2 < 1$. Therefore, the M_1 content of the remaining monomer phase decreases with an increase in the thickness of the copolymer layer. Con-

TABLE I
Monomer Reactivity Ratio

M_1[a]	M_2[a]	r_1	r_2
MMA (1.490)	VPAc (1.567)	22.5	0.005
MMA (1.490)	VB (1.578)	8.52	0.07

[a] Figures in the parentheses represent the refractive index (n_D) of the corresponding homopolymer.

sequently, the resulting rod has a radial distribution in copolymer composition, and the refractive index in the rod decreases with distance r from the center axis. The detailed mechanism of forming a gradient-index distribution was reported elsewhere.[12,13] The copolymer rod with a glass tube was heat-treated at 60–80°C for 20–40 h to polymerize the remaining monomer completely.

Measurement

The index-distribution constant A or A' was calculated by the reduction rate γ of the image formed through the LFR lens. The LFR has the quadratic index distribution expressed as Eq. (1) within radius R_c. The normalized region R_c/R_p was estimated from the size of the image and γ in accordance with the procedure in our previous paper.[10,17] The overall index distribution of LFR was determined from our improved interferometric technique[18] by using Interphako[19] interference microscopy.

The UV absorption spectra of the solutions of the initiators in MMA were measured using UVIDEC-1 spectrophotometer (Japan Spectroscopic Co., Ltd.).

The monomer conversion during the photocopolymerization process was determined gravimetrically as follows: The specimen was dissolved in a small amount of acetone, and the copolymer was precipitated by adding a large amount of methanol, followed by drying *in vacuo* at room temperature.

The temperature of the monomer mixture in a glass tube during UV irradiation was measured by using a copper-constantan thermocouple with a 0.3-mm diameter.

The mixture of MMA/VPAc [=60/40 (w/w)] monomers with BPO (=0.5 wt %) was left at room temperature for 20–30 days and then heat-treated at 70°C for 40 h. The composition of the resulting copolymer bulk was fractionated by a silica–gel column chromatography, using the mixture of ethyl acetate and toluene (80/20–90/10 by volume) as the developer. The composition of the each fraction was analyzed using Varian EM-390 90-MHz NMR spectrometer.

The light scattering from the LFR with a 9-mm diameter was estimated as follows: He–Ne laser (633-nm wavelength) beam was injected on the center of polished end face of the LFR. The light scattering in the direction perpendicular to the incident beam was measured with a Hamamatsu TV R928 photomultiplier tube. To compensate the fluctuation of the intensity of laser beam, the incident ray was splitted by a half-mirror and monitored with a Hamamatsu TV 931-A photomultiplier tube.

RESULTS AND DISCUSSION

Refractive-Index Distribution

In the MMA–VB LFR, the curves for A' value vs. the initiator concentration passed through a max at 2.0 wt % for BPO under MMA/VB = 3.0–5.0 (w/w), and 3.0 wt % for BME under MMA/VB = 5.0 (w/w), respectively. Figure 1 shows the effect of the monomer feed ratio of the MMA–VB LFR on the index-distribution constant A' and the R_c/R_p, when BPO = 2.0 wt % and BME = 3.0 wt %. In the case of the BPO initiation, A' value reached its maximum value at

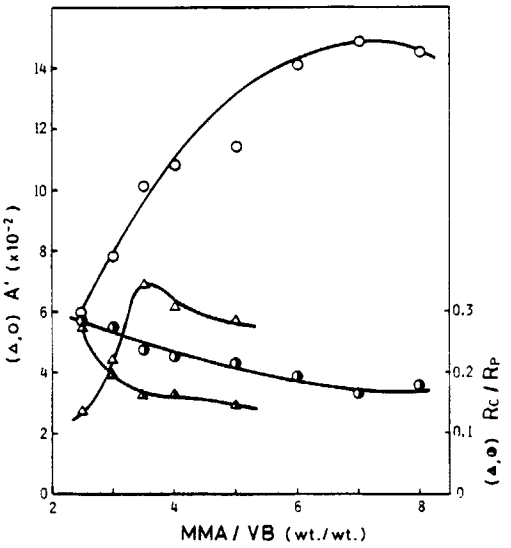

Fig. 1. Effect of monomer feed ratio on A' and R_c/R_p in the MMA–VB LFR, where V = 0.9 mm/min: (△,▲) BPO = 2.0 wt %; (○,●) BME = 3.0 wt %.

MMA/VB = 3.5 (w/w) and R_c/R_p monotonously decreased with an increase in MMA/VB. When using BME as an initiator, the overall trend is similar to that of BPO initiation, but the maximum peak of A' curve was shifted toward the higher MMA content and was twice as high as the maximum A' value by the BPO initiation.

In the MMA–VPAc LFR, the curves for A' value vs. the initiator concentration passed through a max at 0.5 wt % for BPO under MMA/VPAc = 4.0–6.5 (w/w), 1.0 wt % for BN under MMA/VPAc = 6.5, and 3.0 wt % for BME under MMA/VPAc = 6.5, respectively. Figure 2 shows the effect of the monomer feed ratio of the MMA–VPAc LFR on the A' and R_c/R_p, when BPO = 0.5 wt %, BN = 1.0 wt %, and BME = 3.0 wt %, respectively. The overall trends are similar to that of Figure 1 and can be clearly explained by the computer simulation[12,13] on the basis of the mechanism forming an index distribution. It should be noted that in order of BPO, BN, and BME, the maximum A' value increased from 3×10^{-2} to 9×10^{-2}. The above result should be explained by the difference in the

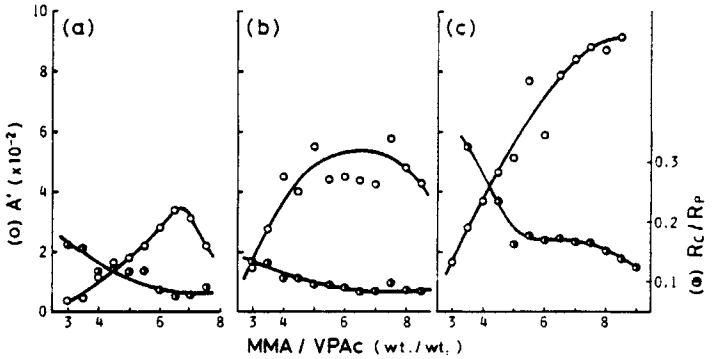

Fig. 2. Effect of monomer feed ratio on A' and R_c/R_p in the MMA–VPAc LFR, where V = 0.9 mm/min: (a) BPO = 0.5 wt %; (b) BN = 1.0 wt %; (c) BME = 3.0 wt %.

photoinitiation rate and the extent of the accompanying thermal polymerization during the photocopolymerization process, detail of which is discussed in the next section.

Figure 3 shows the comparison of the index distribution of the MMA–VPAc LFR by the BPO initiation with that by the BME initiation, which was determined by our interferometry.[18] As the abscissa is $(r/R_p)^2$, eq. (1) is expressed by a straight line. Therefore, the region having a convex lens function corresponds to a linear part of the respective curve in the center region. It is noteworthy that the whole index distribution by the BME initiation is much steeper than that by the BPO initiation.

Effect of the Initiator on the Index Distribution

As shown in Figures 1–3, the refractive-index distribution of the resulting LFR was much affected by the sort of the initiator. In the UV absorption spectra of BPO, BN, and BME in MMA (5×10^{-4} *M*, 10-mm path length), only BME had a considerable absorption band at 340-nm wavelength (ϵ = 157 L·mm^{-1}·M^{-1}), which is consistent with the irradiation band of the used UV lamp. The BN and BPO spectra were found to resemble each other; however, BN had a slightly higher absorption coefficient than BPO in the range of 300–370-nm wavelength. It has been reported[20] that the quantum yields for the radical formation of BME and BN do not differ to any significant extent, and that there is no marked difference in the ability of the resulting radicals to initiate the polymerization. The higher rates of polymerization observed in the presence of BME, compared with BN, may be attributed merely to the greater amount of the light absorbed. It is quite interesting that the order of the ability for photoinitiation, namely BME > BN > BPO, coincides with that of the magnitude of the corresponding A' value in Figure 2.

Figure 4 shows the time-conversion curve for the monomer mixture [MMA/

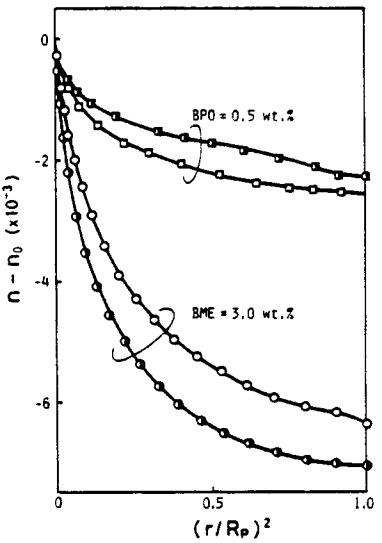

Fig. 3. Comparison of the refractive-index distribution of the MMA–VPAc LFR by BPO initiation with that by BME initiation. MMA/VPAc (w/w): (□,○) 4.0; (■,●) 7.5.

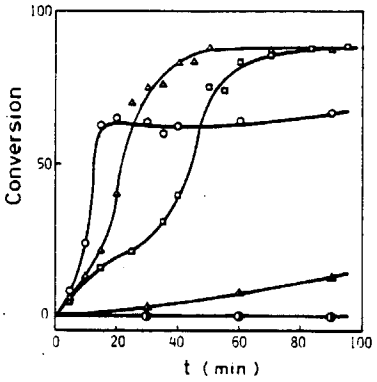

Fig. 4. Time-conversion curves for the photochemical and thermal copolymerization, where MMA/VPAc = 8.0 (w/w): (○,△,□) UV irradiation; (◑,▲) thermal polymn at 50°C; (○,◑) BME = 3.0 wt %; (△,▲) BPO = 3.0 wt %; (□) BPO = 0.5 wt %.

VPAc = 8.0 (w/w)] in a glass tube during the UV irradiation process, along with that for the thermal polymerization at 50°C. The polymerization condition was the same as the fabrication fashion of the LFR except for not moving the UV lamp. When BME = 3.0 wt %, the monomer conversion rapidly increased with the UV irradiation, and the inflection point of the conversion curve appeared at t = 12 min. When using BPO, the polymerization was slowed down in the initial stage, and the inflection point of the conversion curve was shifted to t = 22 min for BPO = 3.0 wt %, and t = 50 min for BPO = 0.5 wt %, respectively. However, the final conversion under the BPO initiation was higher than that of the BME initiation.

Figure 5 shows the temperature change of the MMA–VPAc mixture (8/1 by weight) in the glass tube with the UV irradiation time t, where the chamber was air-cooled at 25°C. Curve S represents the temperature of the same monomer mixture containing hydroquinone (an inhibitor) instead of an initiator. The sample for the curve S after the UV irradiation scarcely contained the polymer. Therefore, the temperature difference of the other sample from the curve S

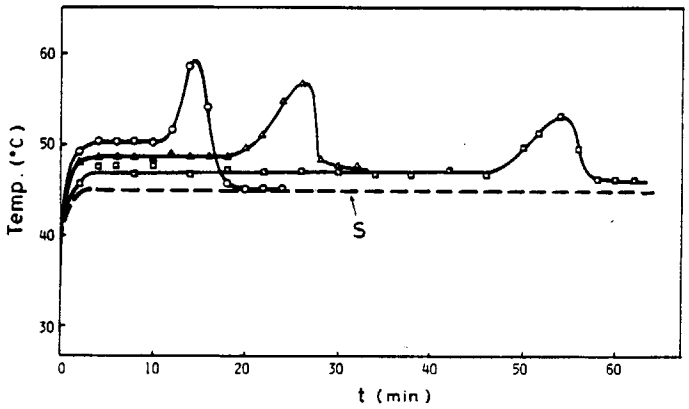

Fig. 5. Temperature change of the MMA/VPAc [=8.0 (w/w)] mixture in a glass tube with a 3-mm diameter, during UV irradiation: (○) BME = 3.0 wt %; (△) BPO = 3.0 wt %; (□) BPO = 0.5 wt %; S, containing hydroquinone without an initiator.

should be attributed only to the heat of polymerization. The maximum peaks for BME and BPO initiation, accompanied with the gel effect, are well consistent with the inflection points of the corresponding conversion curves in Figure 4.

BPO is capable of initiating vinyl polymerization both thermally and photochemically, whereas BME initiates photochemically but not thermally as shown in Figure 4. The refractive-index distribution in the rod is achieved by the initial formation of the copolymer layer on the inner wall of glass tube, detail of which was discussed elsewhere.[12] Therefore, the thermal initiation may be unfavorable for the formation of a gradient-index distribution, because of generating free radicals homogeneously in the entire system. As shown in Figure 5, the temperature of the monomer mixture in the glass tube remarkably increased due to heat generation of the UV lamp, and raised to 46–50°C within 3 min, then went up to 55–59°C at the maximum peak. Therefore, in the case of BPO initiation, it is conceivable that photochemical and thermal initiations occur simultaneously during UV irradiation, and that the concurrent thermal initiation causes a reduction in A' value. On the other hand, the remarkable initial increase in the conversion of BME initiation in Figure 4 implies the rapid formation of the initial copolymer layer on the inner wall of glass tube without thermal initiation. It is concluded that the difference in the index distributions between BPO and BME should be mainly attributed to the above effect for the accompanying thermal initiation during the photocopolymerization process.

The Heterogeneity of the Copolymer Composition

It is predicted from the monomer reactivity ratio in Table I that the copolymer composition in the LFR should be widely distributed. The light scattering loss as well as the index distribution of LFR should be much affected by the dispersion in copolymer composition. In the M_1–M_2 monomer system, the rearranged form of the Mayo–Lewis equation is

$$y = \frac{(r_1 - w)x^2 + wx}{[w(r_2 - 1) + r_1 - 1]x^2 - (2r_2w - w - 1)x + r_2w} \tag{2}$$

where y is the instantaneous weight fraction of M_1 unit in the copolymer when the weight fraction in the monomer mixture is x. Symbol w is the ratio of molecular weight of monomer M_1 to M_2. Assuming that eq. (2) is applicable up to high conversion, the weight conversion P is related to the monomer composition as follows[21]:

$$P = 1 - \left(\frac{x}{x_0}\right)^{\alpha}\left(\frac{x-1}{x_0-1}\right)^{\beta}\left(\frac{x-k}{x_0-k}\right)^{\gamma} \tag{3}$$

where x_0 is the M_1 weight fraction in the monomer feed,

$$\alpha \equiv \frac{r_2}{1-r_2}, \quad \beta \equiv \frac{r_1}{1-r_1}, \quad \gamma \equiv \frac{r_1r_2 - 1}{(1-r_1)(1-r_2)}, \text{ and } k \equiv \frac{w(1-r_2)}{w(1-r_2) + (1-r_1)}$$

Here k corresponds to the critical weight fraction for the azeotrope. Differentiation of eq. (3) yields

$$\frac{dP}{dy} = \frac{dP}{dx}\cdot\frac{dx}{dy} = -\left(\frac{x}{x_0}\right)^{\alpha}\left(\frac{x-1}{x_0-1}\right)^{\beta}\left(\frac{x-k}{x_0-k}\right)^{\gamma}\left(\frac{\alpha}{x} + \frac{\beta}{x-1} + \frac{\gamma}{x-k}\right) \times \frac{[(r_2w + r_1 - w - 1)x^2 - (2r_2w - w - 1)x + r_2w]^2}{(r_1 + r_2w^2 - 2r_1r_2w)x^2 + 2r_2w(r_1 - w)x + r_2w^2} \tag{4}$$

Since $-dP/dy$ corresponds to the amount of the copolymer having the y composition, $-dP/dy$ vs. y curve represents the distribution of copolymer composition.

Figure 6(a) shows the representative distribution curves of composition in the MMA–VPAc and MMA–VB copolymers polymerized completely, which was calculated from eqs. (2) and (4). The distribution curve had the trend to be separated into the two regions close to the corresponding M_1 and M_2 homopolymers. As pointed out graphically by Skeist,[22] when y reaches zero, $-dP/dy$ is simply reduced to be zero, finite value, and infinite for $r_2 > 0.5$, $r_2 = 0.5$, and $r_2 < 0.5$, respectively. Both the MMA–VPAc and MMA–VB copolymer bulks are the case for $r_2 < 0.5$, which means the existence of VPAc and VB homopolymer in the respective LFR.

Johnson et al.[23] studied the constancy of the monomer reactivity ratio in the high conversion copolymerization of styrene with MMA, and showed that the deviation became remarkable with gel effects. On the other hand, several papers[24,25] experimentally showed that the above Meyer's equation, eq. (3), is available up to high conversion. Stejskal and Kratochvil[26] have theoretically confirmed that the so-called statistical composition heterogeneity[27] is negligible in the high molecular weight copolymer. Mirabella and Barrall[28] investigated the composition of poly(styrene-co-vinyl stearate) ($r_1 = 68 \pm 30$ and $r_2 = 0.01 \pm 0.01$, whose values resemble those of MMA–VPAc and MMA–VB copolymers), and confirmed the existence of M_2 homopolymer. In the MMA/VPAc (=60/40 by weight) copolymer bulk, we also observed a considerable amount of the copolymer close to poly(MMA) homopolymer ($0.84 \leq y \leq 0.98$) and the existence of the VPAc homopolymer ($y = 0$) from a silica-gel column chromatography and NMR, which implies that r_2 should be less that 0.5 even near 100% conversion. The recognized amount of the copolymer in the range of $0 < y \leq 0.83$ was not fractionated.

Figure 6(b) shows the effect of the MMA weight fraction x_0 in monomer feed on the distribution of the copolymer composition. With increasing x_0, the U-shaped composition curve spread to the higher MMA composition, lowering the bottom of the U shape and remaining the M_2 homopolymer. The composition

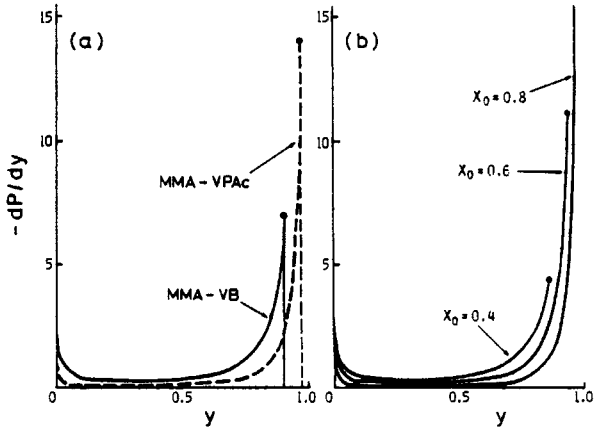

Fig. 6. Distribution of copolymer composition calculated from eqs. (2) and (4): (a) distribution curves for MMA–VB and MMA–VPAc copolymers at $M_1/M_2 = 1.0$ (w/w); (b) effect of the MMA feed composition (x_0) on the composition distribution in MMA–VB copolymer.

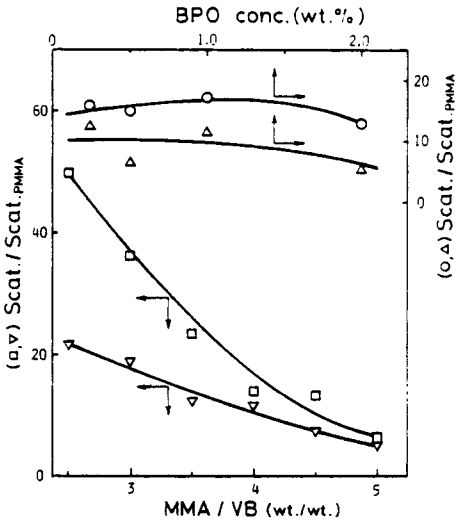

Fig. 7. Light scattering from the MMA–VB LFR with a 9-mm diameter, where V = 0.3 mm/min. MMA/VB (w/w): (○) 4.0; (△) 5.0. BPO concn (wt %): (□) 0.5; (▽) 2.0.

curve angulated at $y \simeq 0$ and $y \simeq 1.0$ implies that the copolymer should be separated into the corresponding M_1 and M_2 homopolymers. It is predicted that, even in the range of the relatively higher x_0, increasing further MMA in monomer feed does not necessarily bring about the reduction in the heterogeneity of the copolymer composition.

Light Scattering

In the copolymer bulk, the light scattering intensity govering the transparency depends on the fluctuation of polarizability attributed to the heterogeneity of the copolymer composition and the density etc. The relative scattering intensity (scat/scat$_{PMMA}$) of the LFR, perpendicular to the incident ray, was measured, employing the intensity of the scattering ray from poly(MMA) bulk as a reference.

Figure 7 shows the effects of the monomer feed ratio and BPO concentration on the relative scattering intensity scat/scat$_{PMMA}$ in the MMA–VB LFR with a 9-mm diameter. The scattering intensity remarkably decreased with MMA/VB from 2.5 to 5.0 (w/w), while scarcely depending on the BPO concentration. Figure 8 shows the scattering intensity in the MMA–VPAc LFR. It should be noted that the levels of the scattering intensities for the MMA–VPAc LFR are one-tenth of those for the MMA–VB LFR in Figure 7. The scattering intensity slightly increased with the BPO concentration. On the other hand, with the monomer feed ratio the scattering intensity had the maximum peak around MMA/VPAc = 6.0 (w/w). As predicted from Figure 6(b), the heterogeneity of copolymer composition at higher x_0 may not be simply reduced by further increasing MMA in monomer feed, which should result in the maximum peak in Figure 8.

The scattering intensity in isotropic polymer materials is given by[29]

$$i = 4\pi\langle\eta^2\rangle V \int_0^\infty \gamma(r) r^2 \frac{\sin(hr)}{hr}\, dr \tag{5}$$

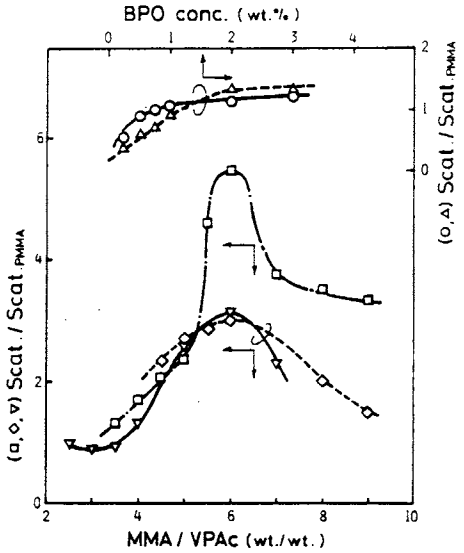

Fig. 8. Light scattering from the MMA–VPAc LFR. V (mm/min): (○,▽) 0.3; (△,□) 0.9; (◇) 1.2. MMA/VPAc (w/w): (○) 3.0; (△) 4.0. BPO concn (wt %): (▽) 0.5; (□,◇) 1.0.

where h is the magnitude of the scattering vector [$h = (4\pi/\lambda)\cdot\sin(\theta/2)$], θ is the scattering angle, λ is the wavelength, V is the scattering volume, $\langle\eta^2\rangle$ is the mean square average of all polarizability fluctuation, and $\gamma(r)$ is the correlation function denoting a measure of the extension of the inhomogeneity in the polymer. As shown in Figure 6, the copolymer composition of the LFR should be separated into the two region close to the M_1 and M_2 homopolymers. Therefore, assuming that the LFR consists of M_1 and M_2 homopolymers, the mean square fluctuation $\langle\eta^2\rangle$ may be expressed as[14,30]

$$\langle\eta^2\rangle = \phi_1\phi_2\left[\frac{9n(n_1 - n_2)}{2\pi(n^2 + 2)^2}\right]^2 \tag{6}$$

where n_1 and n_2 are the refractive indices of the M_1 and M_2 homopolymer phases, n is the average refractive index of the M_1–M_2 polymer blend, and ϕ_1 and ϕ_2 are the corresponding volume fractions. Assuming that the correlation function $\gamma(r)$ for the MMA–VB polymer blend is equal to that for the MMA–VPAc polymer blend, the integral parts of eq. (5) for the above two polymer blends are the same. Here it should be noted that the scattering intensity i is proportional to $\langle\eta^2\rangle$. Therefore, from eq. (6) we can estimate the effect of the index difference between the VB and VPAc homopolymers on the scattering intensity of the respective polymer blend. The calculation at M_1/M_2 = 3.0–8.0 (w/w) showed that the scattering intensity of the MMA–VB polymer blend was only 1.270–1.264 times greater than that of the MMA–VPAc polymer blend. Nevertheless, the experimental data of MMA–VB LFR was about 10 times as large as that of MMA–VPAc LFR in Figures 7 and 8.

In the copolymer bulk consisting of the two regions close to the M_1 and M_2 homopolymers, such as MMA–VPAc and MMA–VB LFRs, the light scattering loss may be much affected by the compatibility of the M_1 and M_2 polymers. In the fabrication of LFR, therefore, the compatibility between the corresponding homopolymers is one of the most important factors for selecting the monomer

pair, as well as the monomer reactivity ratio. The solubility parameter δ of the corresponding homopolymer was calculated according to[31]

$$\delta = \rho \sum G/M \tag{7}$$

where ρ is the density, M is the molecular weight of the monomeric unit, and G is the molar-attraction constant which was estimated from the vapor pressure by Hoy.[31] The calculated solubility parameters of poly(MMA), poly(VPAc), and poly(VB) were 9.3, 10.0, and 10.2 $(cal/cm^3)^{1/2}$, respectively. This shows that the compatibility between MMA and VPAc polymers is superior to that between MMA and VB polymers. Therefore, it is concluded that the difference of the scattering intensity between the MMA–VB and MMA–VPAc LFRs should be attributed to the compatibility of the VPAc and VB polymers to the MMA polymer, and scarcely attributed to the difference of the refractive indices between the VPAc and VB polymers.

CONCLUSIONS

The photocopolymerization of MMA with VB and VPAc, using BPO, BN, and BME as an initiator, was carried out to prepare a light-focusing plastic rod. The LFR with high transparency and steep index distribution was obtained when using the MMA–VPAc monomer pair and the BME which initiates vinyl polymerization photochemically but not thermally. The difference in the index distributions by the BPO, BN, and BME initiations was clarified by considering the rate of the copolymer-layer formation from an inner wall of the glass tube, and the accompanying thermal polymerization during the photocopolymerization process.

The light-scattering intensity from the MMA–VB LFR decreased with increasing the MMA composition in monomer feed. On the other hand, the scattering from the MMA–VPAc LFR had a maximum peak at MMA/VPAc $\simeq$ 6.0 (w/w), which may be ascribed to the heterogeneity of copolymer composition arised at higher MMA composition. On the whole, the scattering intensity from the MMA–VPAc LFR is about one-tenth of that from the MMA–VB LFR, which should be due to the good compatibility between the MMA and VPAc polymers and scarcely due to the index difference between the VPAc and VB polymers.

References

1. D. T. Moore, *Appl. Opt.*, **19**, 1035 (1980).
2. K. Iga, *Appl. Opt.*, **19**, 1039 (1980).
3. K. Matsushita and M. Toyama, *Appl. Opt.*, **19**, 1070 (1980).
4. M. Kawazu and Y. Ogura, *Appl. Opt.*, **19**, 1105 (1980).
5. J. C. Palais, *Appl. Opt.*, **19**, 2011 (1980).
6. W. J. Tomlinson, *Appl. Opt.*, **19**, 1127 (1980).
7. I. Kitano, K. Koizumi, H. Matsumura, T. Uchida, and M. Furukawa, *Suppl. J. Jpn. Soc. Appl. Phys.*, **39**, 63 (1970).
8. Y. Ohtsuka, T. Senga, and H. Yasuda, *Appl. Phys. Lett.*, **25**, 659 (1974).
9. Y. Ohtsuka and T. Senga, *Kobunshi Ronbunshu*, **35**, 721 (1978).
10. Y. Ohtsuka, T. Sugano, and Y. Terao, *Appl. Opt.*, **20**, 2319 (1981).
11. Y. Ohtsuka and Y. Terao, *J. Appl. Polym. Sci.*, **26**, 2907 (1981).
12. Y. Ohtsuka, Y. Koike, and H. Yamazaki, *Appl. Opt.*, **20**, 280 (1981).
13. Y. Ohtsuka and Y. Shimizu, *Kobunshi Ronbunshu*, **35**, 169 (1978).
14. Y. Koike, Y. Kimoto, and Y. Ohtsuka, *Appl. Opt.*, **21**, 1057 (1982).
15. Y. Ohtsuka, Y. Koike, and H. Yamazaki, *Appl. Opt.*, **20**, 2726 (1981).

16. S. R. Sandler, *J. Chem. Eng. Data*, **18**, 445 (1973).
17. Y. Ohtsuka and Y. Koike, *Sen-i Gakkaishi* (*J. Soc. Fiber Sci. Technol. Jpn.*), **37**, 439 (1981), in English.
18. Y. Ohtsuka and Y. Koike, *Appl. Opt.*, **19**, 2866 (1980).
19. Registered trade name of Carl Zeiss, Jena, East Germany.
20. J. Hutchison and A. Ledwith, *Polymer*, **14**, 405 (1973).
21. V. E. Meyer and G. G. Lowry, *J. Polym. Sci. Part A*, **3**, 2843 (1965).
22. I. Skeist, *J. Am. Chem. Soc.*, **68**, 1781 (1946).
23. M. Johnson, T. S. Karmo, and R. R. Smith, *Eur. Polym. J.*, **14**, 409 (1977).
24. H. Inagaki, H. Matsuda, and F. Kamiyama, *Macromol.*, **1**, 520 (1968).
25. S. Teramachi, A. Hasegawa, S. Hasegawa, and T. Ishibe, *Polym. J.*, **13**, 319 (1981).
26. J. Stejskal and P. Kratochvil, *J. Appl. Polym. Sci.*, **25**, 407 (1980).
27. W. H. Stockmayer, *J. Chem. Phys.*, **13**, 199 (1945).
28. F. M. Mirabella, Jr. and E. M. Barrall II, *J. Appl. Polym. Sci.*, **20**, 581 (1976).
29. P. Debye, H. R. Anderson, Jr., and H. Brumberger, *J. Appl. Phys.*, **28**, 679 (1957).
30. J. Koberstein, T. P. Russel, and R. S. Stein, *J. Polym. Sci., Polym. Phys. Ed.*, **17**, 1719 (1979).
31. J. Brandrup and E. H. Immergut, *Polymer Handbook*, Wiley-Interscience, New York, 1975, p. IV–339.

Received November 19, 1981
Accepted February 26, 1982